Asymptotic Numerical Method for Nonlinear Constitutive Laws

Hamid Zahrouni *— Michel Potier-Ferry * — Hassan Elasmar ** Noureddine Damil **

** LPMM, URA CNRS 1215, ISGMP, Université de Metz*
Ile du Saulcy, F-57045 Metz cedex 01
{zahr, potier-ferry}@lpmm.univ-metz.fr

*** Laboratoire de Calcul Scientifique en Mécanique*
Faculté des Sciences Ben M'Sik, Université Haasan II
Sidi Othman, Casablanca, Maroc

ABSTRACT. *This paper deals with the application of the asymptomatic numerical method (ANM) to problems involving nonlinear constitutive laws. We are interested in the deformation theory of plasticity which does not take into account the elastic unloading. We show how to obtain a quadratic form of the problem, what allows us to apply easily the perturbation techniques and to obtain the fastest algorithm. Three constitutive behaviors will be analyzed and some examples will be presented to assess the interest of the proposed algorithm as compared with the classical iterative method of Newton-Raphson.*

RÉSUMÉ. *Nous présentons l'application de la méthode asymptotique numérique (MAN) aux problèmes des structures régies par une loi de comportement non linéaire. Nous nous intéressons à la théorie de déformation totale qui ne prend pas en compte la décharge élastique. Nous montrons comment obtenir une formulation quadratique du problème, ce qui permet d'appliquer simplement une technique de perturbation et d'obtenir l'algorithme le plus rapide possible. Nous étudions trois lois de comportement et nous analysons quelques exemples qui montrent l'intérêt de notre algorithme par comparaison à la méthode de Newton-Raphson.*

KEYWORDS : *perturbation techniques, finite elements method, nonlinear computation, plasticity.*

MOTS-CLÉS : *méthode de perturbation, éléments finis, calcul non linéaire, plasticité.*

Revue européenne des éléments finis. Volume 7 – n° 7/1998, pages 841 à 869

1. Introduction

In this work, we propose to solve problems involving nonlinear constitutive laws by an Asymptotic Numerical Method (A.N.M.). This latter associates the perturbation techniques to numerical ones like the Finite Element Method. It solves a large class of nonlinear problems with two main advantages : the first one concerns computing time which can be reduced significantly by comparison with the classical iterative methods because ANM needs less tangent stiffness matrix decompositions to describe the whole solution branch. The second advantage reports the reliability of this method because it is naturally based on an adaptative step which is computed a posteriori by analyzing the local nonlinearity of the response curve [COC 941][COC 942].

Historically, the association of perturbation techniques to finite element method is due to Thompson and Walker [THO68]. Later, Yokoo et al. [YOK 76] have presented an application of perturbation method to elastic-plastic structures, but with very small step length. Noor et al. [NOO 811] [NOO 80] [NOO 812] have used these techniques to build Rayleigh-Ritz approximation. A comparative study has been designed in favour of iterative methods [RIK 84].

To solve nonlinear problems, industrial codes usually perform incremental-iterative techniques which are based on a linearization of the governing equations [RIK 72] [CRI 83]. These latters are well-adapted to problems with different nonlinearities, but it is difficult to choose the size of the control parameter. If this latter is too small, it induces a large computing time; and if it is too large, the computation diverges. Despite of the adaptative step developed for these techniques, it remains difficult to obtain an optimal step length adapted for each problem (see a comparative study in [ZAH 97]).

Asymptotic numerical method shows an alternative way for a class of nonlinear problems. The efficiency of this method is brought out in several applications for which governing equations are formulated in a quadratic framework. Indeed, these tests concern problems with geometrical nonlinear behavior in the framework of shell structures with moderate rotations [AZR 93], computation of bifurcation points and post-buckling analysis [BOU 94] [VAN 98], solving Navier-Stokes equations [HAJ 95] [TRI 96] [CAD 97]. A computing time study has been performed to compare cubic based formulation and quadratic one. This study advocates the quadratic formulation which permits to reduce CPU time significantly [ZAH 98].

Our group has extended the application field of ANM to problems which involve strong nonlinearity like in plasticity [BRA 95], viscoplasticity [POT 972] [DES 97], unilateral contact [ELH 98].

As these problems involve strong nonlinearity and some singularities, a technique has been proposed to overcome these difficulties and to put the problem into a quadratic form. This technique is based on three simple ideas : first, one regularizes the non-smooth equations [BRA 95]; second, one introduces differential relations when the problem involves power laws [POT 971]; last, one adds new variables to reduce the degree of polynomial relations.

An alternative method to solve such problems is proposed by Ammar [AMM 96] which computes residual vectors directly and not from right hand sides obtained by

series terms. Its algorithm has been presented for large rotations of shells and it seems to be applicable for any kind of nonlinearity.

The aim of this work is to show how to use the asymptotic numerical method for problems which require a nonlinear constitutive law. We shall use techniques given before to obtain a quadratic form of the governing equations allowing us to perform the same algorithm as in elasticity case [COC 942].

2. The classical representation of the A.N.M.

To solve a nonlinear problem in the framework of asymptotic numerical method, we usually perform the procedure described below [COC 942] :

- Choose a quadratic variational formulation like the Hellinger-Reissner one which is expressed in terms of displacement and stress fields as the basic variables.
- Then expand both these variables and the load parameter into power series in the neighbourhood of an initial solution. These developments are then substituted into the variational problem to obtain a sequence of linear problems which have the same tangent operator. The nonlinear terms are reported on right hand side vectors. At this level, we have two equations at each order reporting the equilibrium condition and the elastic constitutive relation.

The most important formulation widely used to compute practical problems is the displacement-based finite element method for its simplicity and its good numerical properties. So at each order, we substitute the constitutive equation into the equilibrium one. We then obtain, at a given order "p", only one equation with the displacement field as unknown. This equation is solved by the displacement-based finite element method. Next, the stress field is deduced from the displacement solution.

Consider a three dimensional elastic problem with a geometric nonlinearity. Variational formulation can be reported by these two equations :

$$\int_v {}^t\mathbf{S} : \delta\gamma(u)\ dv - \lambda P_e(\delta u) = 0 \qquad [1]$$

$$\mathbf{S} = \mathbf{D} : \gamma(u) \qquad [2]$$

where [1] and [2] denote equilibrium condition and constitutive relation respectively. D is the elastic stiffness tensor, u lists the displacement field, λ is a load parameter and λP_e denotes the work done by the external load. S is the second Piola-Kirchoff stress tensor and γ is the Green-Lagrange strain which can be decomposed into a linear part and a quadratic one :

$$\begin{aligned} &\gamma(u) = \gamma_l(u) + \gamma_{nl}(u,u) = \tfrac{1}{2}(\nabla\mathbf{u} + {}^t\nabla\mathbf{u}) + \tfrac{1}{2}({}^t\nabla\mathbf{u}\ \nabla\mathbf{u}) \\ &\delta\gamma(u) = \gamma_l(\delta u) + 2\ \gamma_{nl}(u,\delta u) \end{aligned} \qquad [3]$$

The perturbation techniques allow us to seek a part of the solution branch of the problem ([1] and [2]) by expanding the variables $\mathbf{u}$, $\mathbf{S}$ and λ into power series with

respect to a parameter "a" which represents an additional unknown which is similar to the control parameter of the classical iterative algorithms. Indeed, we can write the variables in the following form:

$$\mathbf{u}(a) = \sum_{i=0}^{p} a^i \mathbf{u}_i \qquad \mathbf{S}(a) = \sum_{i=0}^{p} a^i \mathbf{S}_i \qquad \lambda(a) = \sum_{i=0}^{p} a^i \lambda_i \qquad [4]$$

We can consider the parameter "a" as the projection of the pair $(\mathbf{u} - \mathbf{u}_0, \lambda - \lambda_0)$ on the tangent direction $(\mathbf{u}_1, \lambda_1)$ which corresponds to an arc length parameter for iterative methods. By substituting [4] into [1] and [2] and equating like powers of "a", we obtain a sequence of linear problems that we can write at a given order "p" in the following form:

$$\bullet \int_v \{{}^t\mathbf{S}_p : (\gamma_l(\delta u) + 2\gamma_{nl}(u_0, \delta u)) + {}^t\mathbf{S}_0 : (\gamma_l(u_p) + 2\gamma_{nl}(u_0, u_p))\}\, dv =$$

$$\lambda_p\, \mathbf{F} + \int_v \sum_{r=1}^{p-1} {}^t\mathbf{S}_r : 2\gamma_{nl}(u_{p-r}, \delta u)\, dv \qquad [5]$$

$$\bullet \mathbf{S}_p = \mathbf{D} : \{\gamma_l(u_p) + 2\gamma_{nl}(u_0, u_p) + \sum_{r=1}^{p-1} \gamma_{nl}(u_r, u_{p-r})\} \qquad [6]$$

These equations involve two variables which are the displacement field u_p and the stress one S_p. By substituting [6] into [5], we obtain only one equation whose unknown is u_p. After discretization, this problem can be written as follow:

$$[Kt]\{\mathbf{u}_p\} = \lambda_p\{\mathbf{F}\} + \{\mathbf{F}_p^{nl}\} \qquad [7]$$

where $[Kt]$ denotes the tangent stiffness matrix computed at the initial solution, $\{\mathbf{u}_p\}$ is the discretized displacement vector at order "p". The nonlinear terms are reported on $\mathbf{F}_p^{nl}$ vector; these terms hold displacements and stresses computed at previous orders. At this stage, the linear problems are well-posed and we can proceed to compute displacement vectors at each order until the given order "p". Thus, we obtain a part of the solution branch by decomposing only one matrix $[Kt]$, which is the same for all the linear problems [7].

We have performed this method to reduce the CPU time when solving a given nonlinear problem. The choice of the optimal truncature order "p" of the series is studied in the application section.

We have presented the classical asymptotic numerical algorithm to deal with an elastic problem for which the basic formulation is simply set in quadratic framework. When a strong nonlinearity due to the constitutive relation is required, how to apply the A.N.M. for such a problem? We will answer this question in the next section.

3. Constitutive laws and regularization

In this section, we will present some constitutive laws which can be easily adapted to the ANM algorithm. The elastic unloading is not considered in this study. Indeed, we use the deformation theory of plasticity (Hencky, 1925) which is convenient for the applications where the physical nonlinearity is more important than the effect of the irreversible process and the history of the loading. We propose to analyse three constitutive laws describing an elastic-perfectly plastic behavior, a Ramberg-Osgood model and a linear hardening model.

Asymptotic expansions are not directly applicable to these laws. Firstly, we must regularize these constitutive relations which have some singularities like the abrupt change in the tangent modulus of the elastic-perfectly plastic case. Secondly, the resultant formulation is strongly nonlinear; to obtain a quadratic form, we must introduce additional variables.

In the following, we shall show how to set each model into a quadratic form to make easier the implementation in the ANM context.

3.1. *Elastic-perfectly plastic behavior*

We now present a constitutive law based on an elastic-perfectly plastic behavior. This is an idealisation of the stress-strain response which can be valid for some practical applications. In this case, we neglect material hardening effects and the elastic unloading. By considering the uniaxial behavior, this law can be written as follows:

$$\begin{aligned} \epsilon &= \frac{\sigma}{E} \qquad |\sigma| < \sigma_y \\ \epsilon &= \frac{\sigma}{E} + \epsilon^p \qquad |\sigma| = \sigma_y \end{aligned} \tag{8}$$

where $\epsilon, \sigma, \epsilon^p, E$ and σ_y denote the strain, the stress, the plastic deformation, the Young's modulus and the yield stress respectively.

This stress-strain relation is singular at yield limit; so that the response curve of a structural problem can not be analytic with such a law. For this reason, we propose to replace this relation by an another one which is analytic and well-adapted to asymptotic expansions [BRA 95]. We shall then replace the constitutive law [8] by an hyperbolic one written in the following form:

$$E\,\epsilon = \sigma + \frac{\eta\,\sigma_y^2}{\sigma_y^2 - \sigma^2}\,\sigma \tag{9}$$

Note that this relation involves two branches as shown in figure (1) which relates the stress-strain response. The first branch corresponds to a stress which stands below the yield stress σ_y, it never passes over. For η small, it is close to the elastic-perfectly plastic law [8] and therefore it is physically admissible. In the second branch case, σ is

greater than σ_y and then it is physically not acceptable. In this new constitutive law, η is a regularization parameter. As shown in figure (1), this parameter acts on the slope of the constitutive curve.

This constitutive relation can be generalized to the three-dimensional case in terms of the Green-Lagrange strain field γ and the Piola-Kirchhoff stress field $\mathbf{S}$. By considering large displacements but small deformations, we can choose an additive decomposition of the strain field [GRE 65] [DAM 97]. This model can be written in the following form:

$$E\,\gamma = (1+\nu)\,\mathbf{S}^d - (1-2\nu)\,P\,I + \frac{\eta\,\sigma_y^2}{\sigma_y^2 - S_{eq}^2}\,\mathbf{S}^d \qquad [10]$$

where E, ν and σ_y respectively relate the Young's modulus, the Poisson's ratio and the yield stress. $P = -\frac{1}{3}\mathbf{S} : I$ is the equivalent hydrostatic stress, $S_{eq} = \sqrt{\frac{3}{2}\mathbf{S}^d : \mathbf{S}^d}$ is the Mises equivalent stress, $\mathbf{S}^d = \mathbf{S} + PI$ is the stress deviator and I is the unit matrix.

To set this law in a quadratic framework, it is suffucient to introduce two new scalar variables: $s^{eq} = S_{eq}^2$ and $\zeta = \frac{\eta\,\sigma_y^2}{\sigma_y^2 - s^{eq}}$. The constitutive law is then described by the following equations:

$$\begin{aligned}
&\bullet\quad E\,\gamma = (1+\nu)\,\mathbf{S}^d - (1-2\nu)\,P\,I + \zeta\,\mathbf{S}^d \\
&\bullet\quad \zeta\,(\sigma_y^2 - s^{eq}) = \eta\,\sigma_y^2 \qquad [11] \\
&\bullet\quad s^{eq} = S_{eq}^2 = \frac{3}{2}\,\mathbf{S}^d : \mathbf{S}^d
\end{aligned}$$

3.2. *Elastic-linear hardening model*

The elastic-perfectly plastic behavior is an idealization of the real material behavior because beyond the yield stress, there is generally a hardening effect. For this reason, we consider a more realistic model which takes into account a linear hardening behavior. As for the previous law, we have to regularize this latter to expand it into power series.

One can remark that if we introduce the generalized thermodynamic force as a new variable [MAU 92], we can perform the same regularization adopted in the law studied before. In the elastic range, this force is equal to the stress field; but in the plastic range it remains constant and equal to the yield stress. For more detail about regularization procedure, refer to the appendix (1).

In three-dimensional case, the relation which links stress field $\mathbf{S}$ to the generalized thermodynamic force $\mathbf{A}$ can be written as follows:

$$\mathbf{S} = \mathbf{A} + \frac{h\,\eta\,\sigma_y^2}{E\,(\sigma_y^2 - A_{eq}^2)}\,\mathbf{A}^d \qquad [12]$$

We use then the same hyperbolic relation as in elastic-perfectly plastic behavior which relies the field $\mathbf{A}$ to the Green-Lagrange strain γ :

$$E\,\gamma = (1+\nu)\,\mathbf{A}^d - (1-2\nu)\,P_A\,I + \frac{\eta\,\sigma_y^2}{\sigma_y^2 - A_{eq}^2}\,\mathbf{A}^d \qquad [13]$$

where ν denotes Poisson's ratio, $P_A = -\frac{1}{3}\mathbf{A} : I$, $A_{eq}^2 = \frac{3}{2}\mathbf{A}^d : \mathbf{A}^d$, $\mathbf{A}^d = \mathbf{A} + P_A I$.

To obtain a quadratic form of this law, we have to introduce two additional variables $s^{eq} = A_{eq}^2$ and $\zeta = \frac{\eta\,\sigma_y^2}{\sigma_y^2 - s^{eq}}$. Finally, equations describing the nonlinear constitutive behavior can be written as follows:

$$\begin{aligned}
&\bullet\quad E\,\gamma = (1+\nu)\,\mathbf{A}^d - (1-2\nu)\,P_A\,I + \zeta\,\mathbf{A}^d \\
&\bullet\quad \zeta\,(\sigma_y^2 - s^{eq}) = \eta\,\sigma_y^2 \\
&\bullet\quad s^{eq} = A_{eq}^2 = \frac{3}{2}\,\mathbf{A}^d : \mathbf{A}^d \qquad [14] \\
&\bullet\quad \mathbf{S} = \mathbf{A} + \frac{h}{E}\,\zeta\,\mathbf{A}^d
\end{aligned}$$

3.3. *Elastic-plastic behavior of the Romberg-Osgood model*

In this section, we are interested in a constitutive law based on the Ramberg-Osgood relationship [CHE 94] [ABA 95]. In three-dimensional case, this law is given by the following relation:

$$E\,\gamma = (1+\nu)\,\mathbf{S}^d - (1-2\nu)\,P\,I + \frac{3}{2}\alpha\left[\frac{S_{eq}}{\sigma_y}\right]^{n-1}\mathbf{S}^d \qquad [15]$$

where E, ν, α, n and σ_y relate the Young's modulus, the Poisson's ratio, the yield offset, the hardening exponent and the yield stress respectively.

As the hardening exponent n is not an integer, this law is not analytic for null stress. That is why a regularization procedure is introduced in this model allowing expansions into power series. For this purpose, we can redefine the Mises equivalent stress in the following form:

$${S_{eq}}^2 = \frac{3}{2}\,\mathbf{S}^d : \mathbf{S}^d + \eta^2\,{\sigma_y}^2 \qquad [16]$$

where η denotes a regularization parameter. For $\eta = 0$, one returns to the initial constitutive law.

At this level, the presented law is analytic, but a difficulty remains due to the non-integer exponent n. Braikat [BRA 95] used in his thesis an integer exponent and has limited the truncature order at 6. To avoid this limitation and to obtain a quadratic

framework, we introduce the following variables κ and ζ and we transform the power law into a differential equation [POT 971] [POT 972].

$$\kappa(S_{eq}) = \frac{3}{2}\,\alpha\,\left[\frac{S_{eq}}{\sigma_y}\right]^{n-1} = \frac{3}{2}\,\alpha\,\left[\frac{3}{2\,{\sigma_y}^2}\,\mathbf{S}^d : \mathbf{S}^d + \eta^2\right]^{\frac{n-1}{2}} \qquad [17]$$

$$\zeta^2 = \frac{S_{eq}^2}{\sigma_y^2} = \frac{3}{2\,{\sigma_y}^2}\,\mathbf{S}^d : \mathbf{S}^d + \eta^2 \qquad [18]$$

These two variables are linked as follows:

$$\kappa = \frac{3}{2}\alpha\,\zeta^{n-1} \qquad [19]$$

If we carry out a differenciation of this latter equation, we obtain a relation which is more convenient for the asymptotic expansions:

$$\zeta\,d\kappa = (n-1)\,\kappa\,d\zeta \qquad [20]$$

In this way, we obtain a general problem with a quadratic nonlinearity allowing us to use a similar algorithm as the one developed in elastic studies [COC 942] [ZAH 98]. Moreover, to keep the same initial slope as for non-regularized law, the first member of equation [15] must be multiplied by $(1+\alpha\eta^n)$.

The global structural problem is then formulated by both equilibrium condition and the following equations which represent the constitutive relation and the two additional equations relative to the variables κ and ζ:

$$\begin{aligned}
&\bullet\quad E(1+\alpha\eta^n)\,\gamma = (1+\nu)\mathbf{S}^d - (1-2\nu)PI + \kappa\mathbf{S}^d \\
&\bullet\quad \zeta^2 = \frac{3}{2\,{\sigma_y}^2}\,\mathbf{S}^d : \mathbf{S}^d + \eta^2 \qquad [21] \\
&\bullet\quad \zeta\,d\kappa = (n-1)\,\kappa\,d\zeta
\end{aligned}$$

4. The Asymptotic-Numerical algorithm

4.1. *Problem to be solved*

Since the constitutive laws are well-established, we are now interested in the variational formulation of the structural problem in view to apply the finite element discretization. In three-dimensional framework, the equilibrium condition can be related by the following expression:

$$\int_v {}^t\mathbf{S} : \delta\gamma\,dv - \lambda P_e(\delta u) = 0 \qquad [22]$$

where $\delta\gamma$ is the virtual Green-Lagrange strain, λ denotes a load parameter and $\lambda P_e(\delta u)$ is the virtual work done by external forces. These equilibrium condition and constitutive equations [11], [14] or [21] form the problem to be solved. For these three problems, we will use the identical algorithm as it has been performed in the elasticity case.

4.2. *Perturbation technique*

As the problem is well-posed and variables are specified, we expand the load parameter λ and the mixed vector $\mathbf{U}$ into power series with respect to a path parameter "a" whom we take as an arc length parameter [COC 941]. The mixed vector holds the elementary variables which are represented by $\mathbf{U} = (\mathbf{u}, \mathbf{S}, \zeta, s^{eq})$, $\mathbf{U} = (\mathbf{u}, \mathbf{S}, \zeta, \kappa)$ or $\mathbf{U} = (\mathbf{u}, \mathbf{S}, \mathbf{A}, \zeta, s^{eq})$ respectively for the elastic-perfectly plastic law, the Ramberg-Osgood model or the behavior with linear hardening. We search a part of the solution branch in the neighbourhood of a known solution $(\mathbf{U}_0, \lambda_0)$:

$$\mathbf{U}(a) = \mathbf{U}_0 + a\mathbf{U}_1 + a^2\mathbf{U}_2 + a^3\mathbf{U}_3 + \dots \qquad [23]$$

$$\lambda(a) = \lambda_0 + a\lambda_1 + a^2\lambda_2 + a^3\lambda_3 + \dots \qquad [24]$$

$$a = \langle \mathbf{u} - \mathbf{u}_0, \mathbf{u}_1 \rangle + (\lambda - \lambda_0)\lambda_1 \qquad [25]$$

We substitute these latter equations into equilibrium and constitutive ones. Then, by equating like powers of "a", we obtain a sequence of "p" linear problems, where "p" is the truncature order of the series. At this order, equations relative to the additional variables are substituted in the constitutive equation. Next, the stress is substituted into the equilibrium equation to obtain the unique equilibrium relation with the displacement field as the principal unknown. At order 1, the linear problem corresponds exactly to the linear prediction of the Newton-Raphson algorithm. At order "p", there is a right hand side vector $\mathbf{F}_p^{nl}$ which depends on all elementary variables related by the mixed vector $\mathbf{U}$ and which are computed at previous (p-1) orders.

As compared to an elastic problem, the nonlinear constitutive relation leads to a tangent stiffness tensor noted $\mathbf{D}_t$ needed for computing the tangent stiffness matrix, and to residual terms at order p denoted by $\mathbf{S}_p^{res}$. These quantities are detailed in appendix (2).

4.3. *Finite element discretization*

We have implemented this algorithm in a finite element code using an eight nodes solid element [ELA 97], which is straightforward because of the simplicity of the displacement-strain relation. This latter is not obvious when a shell model is considered, because the relation linking global displacement to generalized stresses is generally complex. A simple way has been presented by Ammar [AMM 96] for elastic

shells with large rotations, it allows ones to estimate the right hand sides $\mathbf{F}_p^{nl}$ from residual vectors. In the present study, we have chosen a shell element [BUC94] allowing us to use a three dimensional constitutive law without condensation and a displacement-strain relation [3] which is quadratic.

As shown in figure (2), the displacement field is related by the following expression:

$$\mathbf{u}(\theta^1, \theta^2, \theta^3) = \mathbf{v}(\theta^1, \theta^2) + \theta^3 \mathbf{w}(\theta^1, \theta^2) \qquad [26]$$

in which $\mathbf{v}$ represents the displacement of the mid-surface and $\mathbf{w}$ is the difference vector between the undeformed and deformed directors. $(\theta^1, \theta^2, \theta^3)$ denote the curvilinear, convected co-ordinates.

Furthermore, this model introduces an additional strain $\tilde{\gamma}$ which is linearly varying in thickness direction and chosen orthogonal to the stress field:

$$\tilde{\gamma} = \theta^3 \tilde{\beta}_{33}(\theta^1, \theta^2) g^3 \otimes g^3 \qquad [27]$$

As we require no interelement continuity for the strain component $\tilde{\beta}_{33}$, a bilinear polynomial is assumed for this variable:

$$\tilde{\beta}_{33} = \alpha_1 + \alpha_2 \xi + \alpha_3 \eta + \alpha_4 \xi \eta \qquad [28]$$

where ξ,η are the standard element co-ordinates. The extra-unknown parameters α_1, α_2, α_3 and α_4 can be eliminated on the element level (see [BUC94]).
Orthogonality condition leads to a compatibility equation written in the following form:

$$\int_v {}^t\mathbf{S}_p : \delta\tilde{\gamma} \, dv = 0 \qquad [29]$$

To obtain details of the implementation, readers can refer to [ZAH 97]. For discretization, we use the classical eight nodes serendipity quadrilateral with reduced integration and five Gauss points throught the thickness direction.

4.4. *Continuation procedure*

As the series have a finite radius of convergence, we apply the continuation procedure proposed by Cochelin [COC 941] to describe the whole solution path in step by step manner. At each step, the maximal value of the path parameter 'a' is defined automatically. Cochelin has proposed two ways to define the validity range of the series. The first one is based on the difference in the displacement at two successive orders which must stay inferior to a given value ϵ_1 :

$$Validity\ range: \ a_{max} = \left(\epsilon_1 \frac{\|\mathbf{u}_1\|}{\|\mathbf{u}_p\|} \right)^{\frac{1}{p-1}} \qquad [30]$$

A second validity range definition is based on the residual vector whose increment must stay approximately below a given value ϵ_2 defined by the user. It has been shown that these two validity range definitions can be considered as more or less equivalent provided the parameter ϵ_1 or ϵ_2 is suitably chosen [ZAH 97]. In the present study, we limit ourselves to the step length defined by the relation [30].

5. Numerical results

We present in this section the numerical simulations of the asymptotic algorithm for solving problems with nonlinear constitutive laws. The Newton-Raphson method will be considered as the numerical reference for all examples studied here. This method is implemented in our code using the regularized laws presented in this work. Usually, the best iterative algorithms proposed by commercial codes use an adaptative step length, even if these algorithms are not always reliable as compared with those using constant step length [ZAH 97]. However, the efficiency of these algorithms strongly depends on the chosen strategy and on the considered physical problem. For this reason, the reference algorithm in this study has a constant step length. We shall compute several tests with different step length using an arc-length strategy.

We present three simple but significant examples, where the nonlinear material behavior effect is relevant. The first one is the simple traction of a plate; the second one concerns a cylindrical shell which allows us to seek the optimal truncature order as regards to the computing time. The third example deals with a traction of a thick plate with a circular cut-out; in this case, we use a solid element to discretize the structure.

5.1. *Simple traction of a plate*

In this first example, we consider the simple traction of a plate with length $L = 10.$, width $l = 1.$ and thickness $h = 1.$

In the case of hyperbolic law of elastic-perfectly plastic behavior, material data are given as follows: $E = 10^5$, $\nu = 0.3$, $\sigma_y = 200$. We first analyse the influence of the parameter η on the number of steps. Thus, in the figure (3) we report the load/displacement response for different values of η. We notice that the more η is large, the more the load/displacement curve is smoothly varying. This tendency has a direct influence on the step number of ANM algorithm. Indeed, we give in figure (4) different results concerning the influence of η as well as that of ϵ_1 on the step number by using a truncature order 15.

Information given by this study is:

- For a fixed ϵ_1, the step number increases when the value of η decreases. This tendency is consistent because the non-linearity becomes stronger by approaching the singularity located at the stress limit.

- For a given η, the step number increases when the value of ϵ_1 decreases. This result is the same as in previous studies [ZAH 98] [ELH 98].

- For $\epsilon_1 = 10^{-2}$ and $\eta = 10^{-2}$, we obtain the good curve until the stress limit from which we switch on the second hyperbolic branch that is not physiqually admissible because the stress passes over σ_y (see figure 5). To avoid this, it is sufficient to require an accuracy parameter ϵ_1 smaller than 10^{-2}. So we obtain good results when we choose the accuracy parameter $\epsilon_1 = 10^{-3}$, whatever the value of η is. Indeed, the relative residual obtained at the end of the computation is less than 10^{-5}. So, to obtain a displacement of 5% of the plate length, only 3 steps are needed when $\eta = 10$ and 9 steps when $\eta = 10^{-2}$.

Now, by considering the computation by Newton-Raphson method, we notice that the number of tangent stiffness matrix decompositions is larger than the asymptotic one. Indeed, we have undertaken 3 computations with different values of arc length noted "s" and a required relative residual of 10^{-3}. To obtain 18 points in the load/displacement curve, it is necessary to take $s = 2$ which implies 34 tangent stiffness matrix decompositions. When $s = 10$, we only obtain 4 points on the whole curve : 3 points on the first linear curve and only one point on all curve left ($\eta = 10^{-2}$).

Now, consider the same application with the Ramberg-Osgood model. The material caracteristics are : ($E = 10^5$, $\nu = 0.3$, $\alpha = 0.5$, $n = 3.5$ and $\sigma_y = 200.$) . Concerning η, this parameter is only introduced to avoid a division by zero at the starting point; we then adopt $\eta = 10^{-2}$. To compare the asymptotic numerical solution to the Newton-Raphson one, we have performed 3 computations with different arc lengths and a relative residual required of 10^{-3}. The ANM computation is performed with a truncature order of 15 and $\epsilon_1 = 10^{-4}$. On figure (7), we have reported the step number and the decomposition number of tangent stiffness matrix Kt for the three iterative computations. So, to obtain 19 points on the curve, iterative algorithm needs 43 decompositions of Kt whereas the ANM solution gives a continuous solution curve with a good residual nearly equal 10^{-5} by requiring only 8 steps.

If we consider the elastic-linear hardening model with material constants ($E = 10^5$, $\nu = 0.3$, $\sigma_y = 200$ and the hardening modulus $h = 10^4$), we obtain the same conclusions as previously. Indeed, in figure (8) and figure (9), we report the load / displacement response and the decomposition number of Kt when Newton-Raphson algorithm is used. To obtain only 8 points on the curve, 41 Kt decompositions are needed within the iterative algorithm and only 10 steps when ANM is used with $\epsilon_1 = 10^{-4}$, $\eta = 10^{-2}$ and a truncature order 15.

5.2. *Plastic buckling of a cylindrical shell with two holes : computation time analysis*

We consider a cylindrical shell with two diametrically opposed rectangular cutouts which are placed in the middle between the two ends (figure 10). It is subjected to a uniform axial compression (elastic study [NOO 811][RIK 84]). Due to the symmetry of this set-up, only one octant of the structure will be considered in the computational model. It is discretized with a regular mesh involving 1830 degrees of freedom.

In this study, we consider the Ramberg-Osgood model ($E = 71122.5$, $\nu = 0.3$,

$\alpha = 0.5, n = 3.5, \sigma_y = 71.1225, \eta = 10^{-2}$) and the elastic-perfectly plastic behavior ($E = 71122.5, \nu = 0.3, \sigma_y = 100, \eta = 10^{-1}$).

A crucial information to analyse the efficiency of ANM for a given application is the ratio between the computing time to evaluate the right hand sides and the one needed to evaluate and to decompose the tangent stiffness matrix [AZR 93] [COC 941] [ZAH 97]. If this ratio is sufficiently small, the optimal truncature orders are large and the ANM is efficient for the considered class of problems. This information is presented in figures (11) and (12) as well as the steps number and the total relative time denoting the ratio between the CPU time and time needed for a simple Newton-Raphson prediction.

This study allows us to establish the optimal truncature order of the series. We use an accuracy parameter based on the displacement criterion ($\epsilon_1 = 10^{-4}$). The computation stops when the deflection of the node M reaches 10 mm for the power law and 8 mm for the hyperbolic one, which corresponds to a displacement just after the maximal load point (see figures 13 and 14).

We observe that the optimal truncature order is 10 for the two laws, while it is established at 15 in the elastic case [ZAH 97] [ZAH 98]. This tendency is consistant because in both elastic and plastic cases, the tangent stiffness matrix has the same size, but in the plastic case, the r.h.s. are more intricate because of the material nonlinearity, which leads to an additional computation effort.

Another interesting remark concerns the step number. Indeed, this latter decreases when the truncature order increases in the hyperbolic law case, which is consistant because a large truncature order improves the validity range of the ANM solution. But in the power law case, the step number increases from order 15. This can be due to the weak regularization of the power law which induces small divisors in the perturbation technique.

The time ratio of F^{nl}/Kt is practically the same for the two laws because in the two cases, we decompose a matrix having the same size and we compute a vector F^{nl} requiring the same computation effort. By comparing this ratio with the one obtained in the elastic study, at order 10 for example, we notice that a plastic step requires only an increase of 16% as compared with an elastic step for the same problem.

5.3. *Traction of a thick plate with a circular cut-out*

We consider in this example a square thick plate (100x100) with a circular cut-out (R = 40) and a thickness of 20. Due to the symmetry of the problem, only one octant of the structure will be considered in this study.

We consider the Ramberg-Osgood model with the following caracteristics ($E = 10^5, \nu = 0.3, \alpha = 0.5, n = 3.5, \sigma_y = 200., \eta = 10^{-2}$). The mesh described in figure (15) involves 1080 solid elements and 4836 d.o.f.

This test is performed to assess numerical results of the proposed algorithm for a

problem requiring solid elements. A comparison with Abaqus code is performed : this latter uses the same constitutive law without regularization and an algorithm with an adaptative step. To obtain a displacement of 5 mm of the point B (figure 15), Abaqus needs 14 steps and 40 decompositions of the tangent stiffness matrix with a relative residual of 10^{-3} at each step end. The same computation involves 18 steps that is to say 18 decompositions when asymptotic numerical method is used with a truncature order 15 and an accuracy parameter of 10^{-5}. In this case the relative residual stays below 10^{-5}. Response curve is described in figure (18).

6. Concluding remarks

We have presented in this work an Asymptotic Numerical Method for solving problems using nonlinear constitutive laws. We have limited ourselves to the deformation theory of plasticity which is convenient for some practical applications where the loading history is not important. We have shown that it is possible and easy to implement a nonlinear constitutive law. Furthermore, by judiciously introducing additional variables, we can use the same algorithm as in the elasticity [COC 942] [ZAH 97]. This algorithm remains reliable and optimal because it applies the same continuation procedures as for the elastic case [COC 941].

We have also discussed the CPU time by analyzing the number of tangent stiffness matrix decompositions. We have compared the results obtained by A.N.M. to those found by iterative Newton-Raphson method. This study advocates the asymptotic numerical method. The three considered examples show that we must choose a sufficiently small value of the accuracy parameter ϵ_1 (below 10^{-3}) depending on the problem to be solved.

This choice allows us to avoid a bad residual and to follow bad solutions when the elastic-perfectly plastic and elastic-linear hardening behaviors are used.
With a weak increasing of the required memory, we have formulated the problem within a quadratic framework allowing us to quicken the algorithm. Indeed, the example of cylindrical shell with 1830 d.o.f. shows that the computation of an asymptotic step in plasticity requires only 16% more computing time than one obtained in the elastic study.

The optimal truncature order is about 10. For the same example, the elastic study gives a larger optimal truncature order of 15. The difference between the two tests is not surprising because in both cases, we have a tangent stiffness matrix with the same size to be decomposed, however in nonlinear law case, the right hand side F^{nl} requires more computing time.

For the class of problems considered in this work, A.N.M. is proved more efficient than the Newton-Raphson method. Indeed, less tangent stiffness matrix decompositions are needed; furthermore, A.N.M. is reliable and easy to use because the asymptotic steps are automatically adapted depending on the local nonlinearity of the response path.

Finally, note that all algorithms which improve the validity range of the asymp-

totic representation like Padé approximants can be easily adapted in the present case [NAJ 98].

Bibliographie

[ABA 95] ABAQUS , *Theory and users' manuals (version 5.5)*. Hibbitt, Karlsson and Sorenson, Inc., 1080 Main Street, Pawtucket, RI 02860, USA, 1995.

[AMM 96] AMMAR S., Méthode asymptotique numérique perturbée appliquée à la résolution des problèmes non linéaires en grande rotation et grand déplacement. Thèse, Université Laval, Québec, 1996.

[AZR 93] AZRAR L., COCHELIN B., DAMIL N., POTIER-FERRY M., An asymptotic-numerical method to compute the post-buckling behaviour of elastic plates and shells. *Int. J. Numer. Meth. Eng.*, vol. 36, p. 1251–1277, 1993.

[BOU 94] BOUTYOUR E.H., Méthode Asymptotique-Numérique pour le calcul de bifurcations: Application aux structures élastiques. Thèse, Université de Metz, France, 1994.

[BRA 95] BRAIKAT B., Méthode asymptotique-numérique et fortes non-linéarités. Thèse, Université Hassan II, Casablanca, 1995.

[BRA 97] BRAIKAT B., DAMIL N., POTIER-FERRY M., Méthode asymptotiques numériques pour la plasticité. *Revue Européenne des Eléments Finis*, vol. 6, p. 337–357, 1997.

[BUC94] BÜCHTER N., RAMM E., ROEHL D., Three dimensional extension of non-linear shell formulation based on the Enhanced Assumed Strain Concept. *Int. J. Numer. Meth. Eng.*, vol. 37, p. 2551–2568, 1994.

[CAD 97] CADOU. J.M., Méthode asymptotique numérique pour le calcul des branches solutions et des instabilités dans les fluides et pour les problèmes d'interaction fluide-structure. Thèse, Université de Metz, 1997.

[CHE 94] CHEN W.F., *Constitutive Equations for Engineering Materials*. Elsevier, 1994. Volume 2: Plasticity and modelling.

[COC 941] COCHELIN B., A path-following technique via an asymptotic-numerical method. *Comp. and Struct.*, vol. 53, p. 1181–1192, 1994.

[COC 942] COCHELIN B., DAMIL N., POTIER-FERRY M., The asymptotic-numerical method: an efficient perturbation technique for non-linear structural mechanics. *Revue Européenne des Eléments Finis*, vol. 3, p. 281–297, 1994.

[CRI 83] CRIESFIELD M.A. , An arc-length method including line search and acceleration. *Int. J. Numer. Meth. Eng.*, vol. 19, p. 1269–1289, 1983.

[DAM 97] DAMJANIĆ F.B., BRANK B., PERIĆ D., Elasto-plasticity in the non-linear thin shell modelling. *Computational plasticity, Fundamentals and Applications*, vol. 1, p. 1890–1897. D.R.J. Owen, E. Oñate and E. Hinton (Eds.), Barcelona 1997.

[DES 97] DESCAMPS J., CAO H.-L., POTIER-FERRY M., An asymptotic numerical method to solve large strain viscoplastic problems. *Computational plasticity, Fundamentals and Applications*, D.R.J. Owen, E. Oñate and E. Hinton (Eds.), Barcelona 1997. vol. 1, p. 393–400, 1997.

[ELA 97] ELASMAR H., Calcul des structures plastiques par la Méthode Asymptotique Numérique. Thèse, Université Hassan II, Casablanca, 1997.

[GRE 65] GREEN A.E., NAGHDI P.M., A general theory of an elastic-plastic continuum. *Arch. Rat. Mech. Anal.*, vol. 18, p. 251–281, 1965.

[HAJ 95] HADJI S., Méthodes de résolution pour les fluides incompressibles. Thèse, Université de Technologie de Compiègne, 1995.

[ELH 98] ELHAGE HUSSEIN A., DAMIL N., POTIER-FERRY M., An asymptotic numerical algorithm for frictionless contact problems. *Revue Européenne des Eléments Finis*, vol. 7, n° 1-2-3, p. 119–130, 1998. Hermès, Paris.

[MAU 92] MAUGIN G.A., *The Thermomechanics of Plasticity and Fracture*. Cambridge University Press, 1992.

[NAJ 98] NAJAH A., COCHELIN B., DAMIL N., POTIER-FERRY M., A critical review of asymptotic numerical methods. *Archives of Computational Methods in Engineering*, vol. 5, n° 1, p.31–50, 1998.

[NOO 80] A.K. NOOR, J.M. PETERS., Reduced basis technique for nonlinear analysis of structures. *AIAA Journal*, vol. 18, n° 4, 1980. Article No. 79-0747R.

[NOO 811] NOOR. A.K., Recent advances in reduction methods for nonlinear problems. *Computers and Structures*, vol. 13, p. 31–44, 1981.

[NOO 812] A.K. NOOR, J.M. PETERS., Tracing post-limit-point paths with reduced basis technique. *Comp. Meth. Appl. Mech. Eng.*, vol. 28, p. 217–240, 1981.

[POT 971] POTIER-FERRY M., DAMIL N., BRAIKAT B., DESCAMPS J., CADOU J.M., CAO H.L., ELHAGE HUSSEIN A., Traitement des fortes non-linéarités par la méthode asymptotique numérique. C. R. Acad. Sci. Paris, t.324, Série II b, p.171–177, 1997.

[POT 972] POTIER-FERRY M., CAO H.L., DESCAMPS J., N. DAMIL , An asymptotic numerical method for numerical analysis of large deformation viscoplastic problems. *Computers and Structures*, submitted.

[RIK 72] RIKS E., The application of Newton's method to the problem of elastic stability. *Journal of Applied Mechanics*, vol. 39, p. 1060–1066, 1972.

[RIK 84] RIKS E., Some computational aspects of the stability analysis of nonlinear structures. *Comp. Meth. Appl. Mech. Eng.*, vol. 47, p. 219–259, 1984.

[THO68] J.M.T. THOMPSON , A.C. WALKER., The non-linear perturbation analysis of discrete structural systems. *Int. J. Solids Structures*, vol. 4, p. 757–768, 1968.

[TRI 96] TRI A. , COCHELIN B. , POTIER-FERRY M. , Résolution des équations de Navier-Stokes et détection des bifurcations stationnaires par une Méthode Asymptotique Numérique. *Revue Européenne des Eléments Finis*, vol. 5, p. 415–442, 1996.

[VAN 98] VANNUCCI P., COCHELIN B., DAMIL N., POTIER-FERRY M., An asymptotic-numerical method to compute bifurcating branches. *Int. J. Numer. Meth. Eng.*, vol. 41, p.1365–1389, 1998.

[YOK 76] YOKOO Y., NAKAMURA T., UETENI K., The incremental perturbation method for large displacement analysis of elastic-plastic structures. *Int. J. Numer. Meth. Eng.*, vol. 10, p. 503–525, 1976.

[ZAH 98] ZAHROUNI H., Méthode asymptotique numérique pour les coques en grandes rotations. Thèse, Université de Metz, France, 1998.

[ZAH 97] ZAHROUNI H., COCHELIN B. , POTIER-FERRY M. , Computing finite rotations of shells by an asymptotic-numerical method. *Comp. Meth. Appl. Mech. Eng.*, 1997. to appear.

Article reçu le 25 mai 1998.
Version révisée le 30 septembre 1998.

7. Appendix 1

In this section, we will present how to regularize the elastic-linear hardening model studied in this paper. First, we can define the plastic strain ϵ^p and the generalized thermodynamic force A as follows [MAU 92]:

$$\epsilon^p = \epsilon - \frac{\sigma}{E}$$

$$A = \sigma - h\,\epsilon^p \qquad [31]$$

where E and h denote respectively the Young modulus and the hardening one. The admissible stresses are such that $|A| \leq \sigma_y$ and the constitutive relations are expressed as:

$$\begin{aligned} &\epsilon^p = 0 && if \quad |A| < \sigma_y \\ &A = \sigma_y && if \quad \epsilon^p > 0 \\ &A = -\sigma_y && if \quad \epsilon^p < 0 \end{aligned} \qquad [32]$$

At this level, we obtain the same equations as for the elastic-perfectly plastic behavior. So, we propose to regularize this law by an hyperbolic relation which links the plastic strain ϵ^p to the generalized thermodynamic force A. This relation can be written as:

$$E\,\epsilon^p = \frac{\eta\,\sigma_y^2}{\sigma_y^2 - A^2}\,A \qquad [33]$$

When A is computed, we can deduce the stress σ by using the relation $\sigma = A + h\,\epsilon^p$. In this way, by comparison with elastic-perfectly plastic law, we perform the same regularization procedure and we have an additional equation which links the stress field to the generalized thermodynamic force A. The constitutive equations can be summarized as follows:

$$E\,\epsilon = A + \frac{\eta\,\sigma_y^2}{\sigma_y^2 - A^2}\,A \qquad [34]$$

$$\sigma = A + \frac{h\,\eta\,\sigma_y^2}{E\,(\sigma_y^2 - A^2)}\,A \qquad [35]$$

We can generalize this law to the three-dimensional case by using the Green-Lagrange strain field γ and the Piola-Kirchhoff stress field $\mathbf{S}$. This leads to relations [12] [13].

By introducing two new variables, the constitutive relations can be easily written in the quadratic form 14.

8. Appendix 2

In the preceding sections, we have developed the asymptotic numerical algorithm for problems involving nonlinear constitutive laws. By comparison with the elastic case, we have replaced the elastic stiffness tensor $\mathbf{D}$ by the tangent modulus one $\mathbf{D}_t$ to compute the tangent stiffness matrix K_t. Furthermore, because of these nonlinear laws, stress field involves, at order 'p', residual vector $\mathbf{S}_p^{res}$. This latter leads to additional terms in the right hand side $\mathbf{F}_p^{nl}$. In the present section, we give for each law the expression of $\mathbf{D}_t$ and $\mathbf{S}_p^{res}$.

8.1. *Regularized elastic-perfectly plastic law*

At order 1, we can write the constitutive relation in the following form :

$$\mathbf{S}_1 = \mathbf{D}_t : \gamma_1 \qquad [36]$$

One can show easily that this equation is provided from the expression detailed below :

$$\mathbf{S}_1 = C_1\ \gamma_1 + C_2\ (\gamma_1 : I)\ I + C_3\ (\gamma_1 : \mathbf{S}_0^d)\ \mathbf{S}_0^d \qquad [37]$$

$$\mathbf{S}_1 = \left[C_1\ \Im + C_2\ I \otimes I + C_3\ \mathbf{S}_0^d \otimes \mathbf{S}_0^d\right]\ :\ \gamma_1 \qquad [38]$$

where $\Im$ is the fourth-order identity tensor and C_1, C_2 and C_3 are constants defined as follows :

$$C_1 = \frac{E}{1+\nu+\zeta_0}$$

$$C_2 = \frac{E(\nu + \frac{\zeta_0}{3})}{(1-2\nu)(1+\nu+\zeta_0)}$$

$$C_3 = \frac{-3\ \zeta_0\ E}{(1+\nu+\zeta_0)[(1+\nu+\zeta_0)(\sigma_y^2 - s_0^{eq}) + 3\ \zeta_0\ \mathbf{S}_0^d : \mathbf{S}_0^d]}$$

At order 'p', the constitutive relation is expressed as :

$$\mathbf{S}_p = \mathbf{D}_t : \gamma_p + \mathbf{S}_p^{res} \qquad [39]$$

Matrix $\mathbf{D}_t$ is the same at each order; however, residual stresses are expressed at order 'p' as follows :

$$\mathbf{S}_p^{res} = \frac{1}{1+\nu+\zeta_0}\left[C_4\left[\vartheta\ \mathbf{S}_0^d : \mathbf{S}_0^d + (\sum_{r=1}^{p-1}\zeta_r \mathbf{S}_{p-r}^d)\ :\ \mathbf{S}_0^d\right] - \vartheta\right]\ \mathbf{S}_0^d - \frac{1}{1+\nu+\zeta_0}\sum_{r=1}^{p-1}\zeta_r \mathbf{S}_{p-r}^d$$

where

$$C_4 = \frac{3\ \zeta_0}{(1+\nu+\zeta_0)(\sigma_y^2 - s_0^{eq}) + 3\ \zeta_0\ \mathbf{S}_0^d : \mathbf{S}_0^d}$$

$$\vartheta = \frac{1}{\sigma_y^2 - s_0^{eq}}\left[\frac{3\ \zeta_0}{2}\sum_{r=1}^{p-1}\mathbf{S}_r^d : \mathbf{S}_{p-r}^d + \sum_{r=1}^{p-1}\zeta_r\ s_{p-r}^{eq}\right]$$

8.2. *Regularized elastic-plastic law of the Ramberg-Osgood model*

In the case of the present law, we obtain the same expressions as in equations [36] and [39] but with different values of the constants C_1, C_2 and C_3 :

$$C_1 = \frac{E\ (1+\alpha\ \eta^n)}{1+\nu+\kappa_0}$$

$$C_2 = \frac{(3\ \nu + \kappa_0)\ C_1}{3\ (1-2\ \nu)}$$

$$C_3 = \frac{-K\ C_1}{1+\nu+\kappa_0 + K\ \mathbf{S}_0^d : \mathbf{S}_0^d}$$

where

$$K = \frac{3\,(n-1)\,\kappa_0}{2\,\sigma_0^2\,\zeta_0^2}$$

At order 'p', residual stresses are written in the form below:

$$\mathbf{S}_p^{res} = \frac{1}{1+\nu+\kappa_0}\left[C_5\left[\vartheta\,\mathbf{S}_0^d : \mathbf{S}_0^d + (\sum_{r=1}^{p-1}\kappa_r \mathbf{S}_{p-r}^d) \;:\; \mathbf{S}_0^d\right] - \vartheta\right]\mathbf{S}_0^d - \frac{1}{1+\nu+\kappa_0}\sum_{r=1}^{p-1}\kappa_r \mathbf{S}_{p-r}^d$$

where

$$C_5 = \frac{K}{1+\nu+\kappa_0+K\,\mathbf{S}_0^d : \mathbf{S}_0^d}$$

$$\vartheta = \sum_{r=1}^{p-1}\frac{(p-r)(n-1)-r}{p\,\zeta_0}\zeta_{p-r}\kappa_r + \frac{3\,(n-1)\,\kappa_0}{4\,\sigma_0^2\,\zeta_0^2}\sum_{r=1}^{p-1}\mathbf{S}_r^d : \mathbf{S}_{p-r}^d - \frac{(n-1)\,\kappa_0}{2\,\zeta_0^2}\sum_{r=1}^{p-1}\zeta_r\zeta_{p-r}$$

8.3. *Regularized elastic-linear hardening law*

For the present law, we have performed the same regularization procedure as with the elastic-perfectly plastic material. The constitutive law is related by the following equations:

- $E\,\gamma = (1+\nu)\,\mathbf{A}^d - (1-2\nu)\,P_A\,I + \zeta\,\mathbf{A}^d$ [40]
- $\mathbf{S} = \mathbf{A} + \dfrac{h}{E}\,\zeta\,\mathbf{A}^d$ [41]

Equation [40] allows ones to write, at order 'p', this relation:

$$\mathbf{A}_p = \overline{\mathbf{D}_t} : \gamma_p + \mathbf{A}_p^{res} \qquad [42]$$

This expression is identical to that met in the elastic-perfectly plastic case. $\overline{\mathbf{D}_t}$ lists exactly the $\mathbf{D}_t$ matrix of equation [39]. $\mathbf{A}_p^{res}$ has the same expression of $\mathbf{S}_p^{res}$ reported by equation [39] where $\mathbf{S}$ is replaced by $\mathbf{A}$.

To obtain the tangent modulus matrix, we use relation [41] which gives $\mathbf{S}$ as a function of $\mathbf{A}$:

$$\mathbf{S}_p = (1+\frac{h}{E}\zeta_0)\,\mathbf{A}_p + \frac{3\,\zeta_0\,h}{E\,(\sigma_0^2 - s_0^{eq})}\,(\mathbf{A}_0^d : \mathbf{A}_p)\mathbf{A}_0^d - \frac{h\,\zeta_0}{3\,E}\,(\mathbf{A}_p : I)I + \overline{\mathbf{S}}_p^{res} \qquad [43]$$

where

$$\overline{\mathbf{S}}_p^{res} = \frac{h}{E}\sum_{r=1}^{p-1}\zeta_r \mathbf{A}_{p-r}^d + \frac{h}{E\,(\sigma_0^2 - s_0^{eq})}\left[\frac{3\,\zeta_0}{2}\sum_{r=1}^{p-1}\mathbf{A}_r^d : \mathbf{A}_{p-r}^d + \sum_{r=1}^{p-1}\zeta_r s_{p-r}^{eq}\right]\mathbf{A}_0^d \qquad [44]$$

We can rewrite equation [43] in the following form:

$$\mathbf{S}_p = \overline{\mathbf{A}} : \mathbf{A}_p + \overline{\mathbf{S}}_p^{res} \qquad [45]$$

where $\overline{\mathbf{A}}$ is a fourth-order tensor.

By substituting equation [42] into [45], we obtain the constitutive relation expressed as:

$$\mathbf{S}_p = \overline{\mathbf{A}} \otimes \overline{\mathbf{D}_t} : \gamma_p + (\overline{\mathbf{A}} \otimes \mathbf{A}_p^{res} + \overline{\mathbf{S}}_p^{res}) = \mathbf{D}_t : \gamma_p + \mathbf{S}_p^{res} \qquad [46]$$

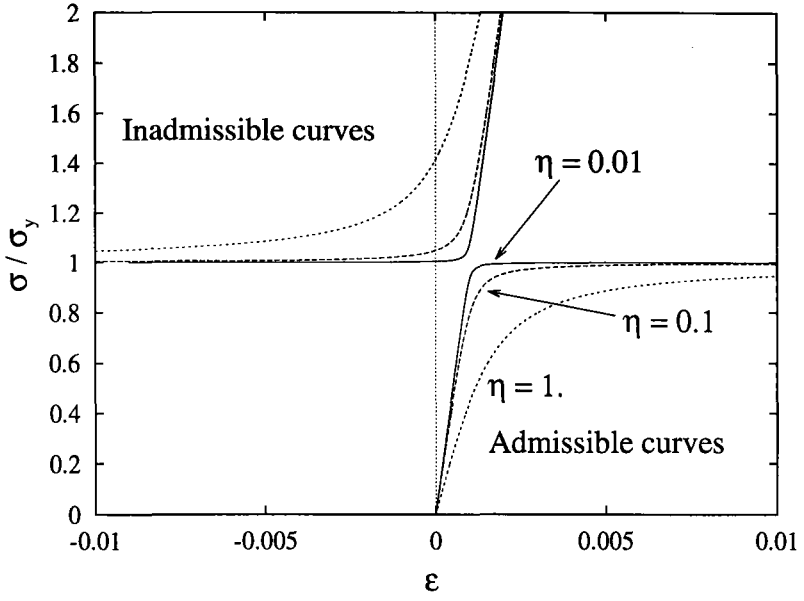

Figure 1. *Simple traction : regularized elastic-perfectly plastic law with different values of η*

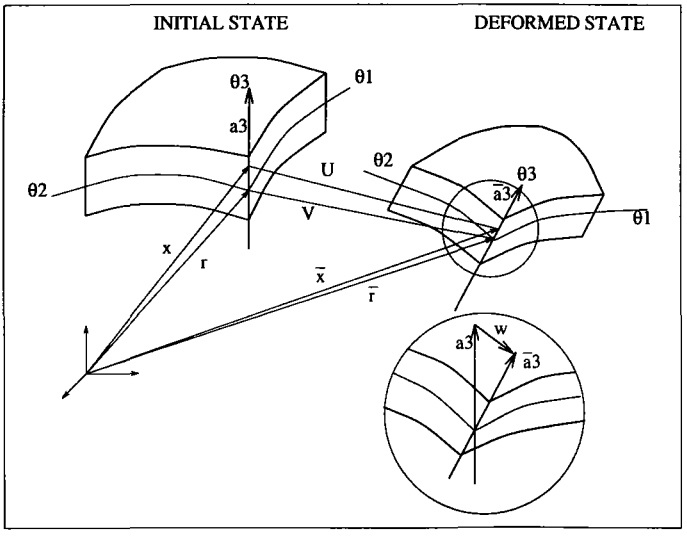

Figure 2. *Shell geometry and kinematic*

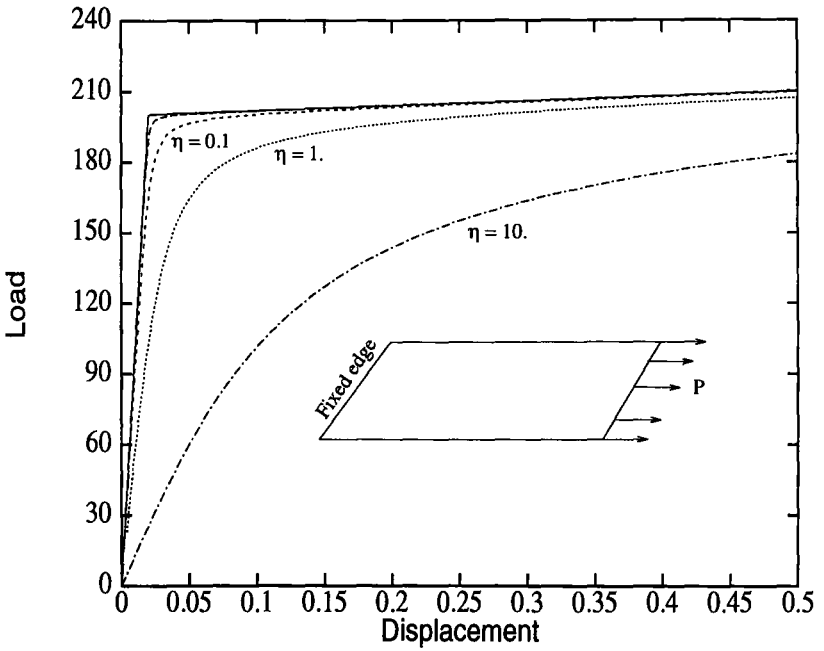

Figure 3. *Regularized elastic-perfectly plastic law: load-displacement curve of a loaded node, with different values of* η*, for simple traction of a beam*

Asymptotic numerical method (order p=15)					
ϵ_1	η	10.	1.	0.1	0.01
10^{-2}	Step number	2	4	6	**
	Residual (log_{10})	-3.9	-4.3	-3.9	**
10^{-3}	Step number	3	5	7	9
	Residual (log_{10})	-5.6	-5.4	-6.9	-5.7
10^{-4}	Step number	3	6	9	11
	Residual (log_{10})	-7.1	-6.4	-7.6	-6.6
10^{-5}	Step number	4	7	11	14
	Residual (log_{10})	-7.2	-7.3	-7.4	-7.2
10^{-6}	Step number	4	9	13	17
	Residual (log_{10})	-8.1	-7.4	-8.0	-7.6
Newton-Raphson method					
$s = 2.$	Step number	16	18	18	18
	Nb decomp. Kt	58	58	47	34
$s = 5.$	Step number	7	7	7	7
	Nb decomp. Kt	27	27	23	16
$s = 10.$	Step number	4	4	4	4
	Nb decomp. Kt	19	18	16	14

Figure 4. *Regularized elastic-perfectly plastic law: influence of η and ϵ_1 on the number of tangent stiffness matrix decompositions. The quality of the approximation of the solution is measured by the decimal logarithm of the relative residual norm vector*

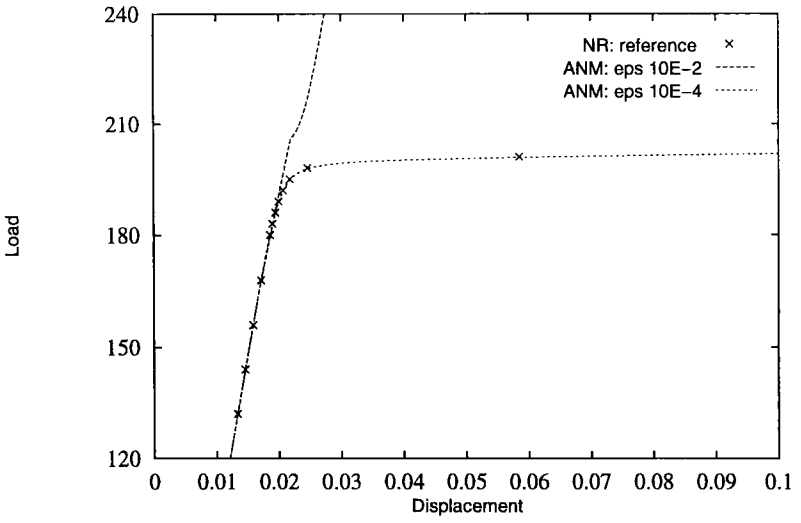

Figure 5. *Regularized elastic-perfectly plastic law: load-displacement curve for simple traction of a beam; comparison between iterative solution and ANM one*

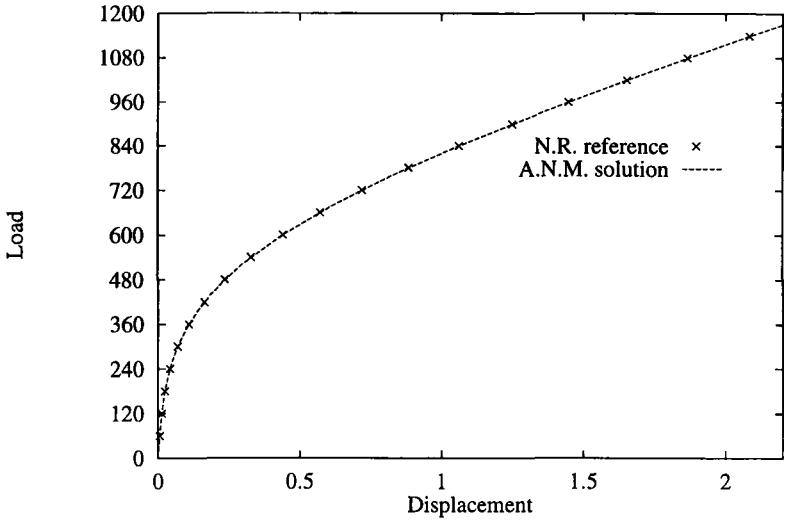

Figure 6. *Regularized Ramberg-Osgood model: load-displacement curve for simple traction of a beam; comparison between iterative solution (s=10) and ANM one*

Newton-Raphson			
	s = 1.	s = 5.	s = 10.
Step number	187	38	19
Number of decomp. Kt	320	87	43

Figure 7. *Regularized Ramberg-Osgood model, simple traction of a beam: analysis of the number of tangent stiffness matrix decompositions with respect to the imposed arc length with Newton-Raphson algorithm (the maximal relative residual allowed is* 10^{-3}*)*

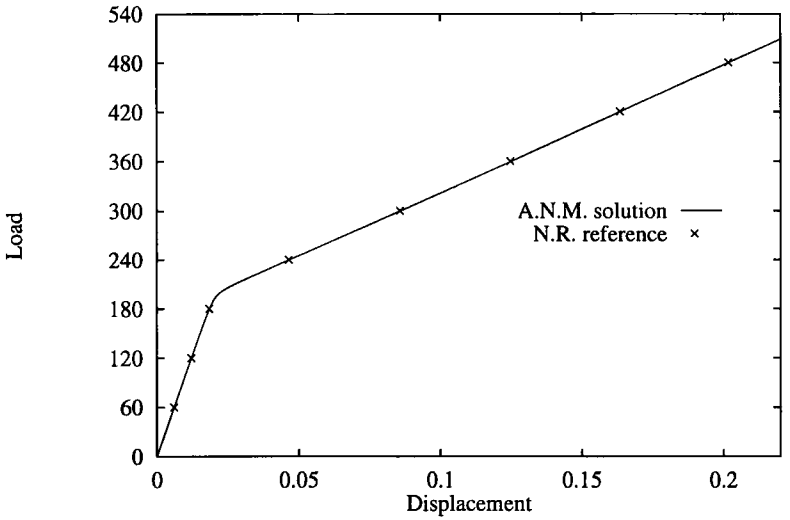

Figure 8. *Regularized elastic-linear hardening law: load-displacement curve with different values of η for simple traction of a beam; comparison between iterative solution (s=10) and ANM one*

Newton-Raphson			
	s = 1.	s = 5.	s = 10.
Step number	80	16	8
Number of decomp. Kt	241	72	41

Figure 9. *Regularized elastic-linear hardening law, simple traction of a beam: analysis of the number of tangent stiffness matrix decompositions with respect to the imposed arc length with Newton-Raphson algorithm (the maximal relative residual allowed is 10^{-3})*

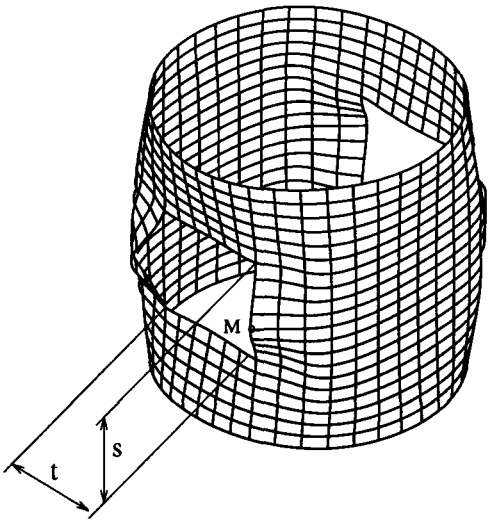

Geometry :
L = 200. mm
R = 100. mm
h = 1. mm
s = 80. mm
t = 79.5 mm

Material :
E = 71122.5 Mpa
ν = 0.3

Figure 10. *Deformed configuration of cylindrical shell under axial and uniform pressure P=981. N/mm*

Truncature order	5	8	10	15	20	30
Step number	44	24	21	20	20	22
$\frac{Fnl\ evaluation}{Kt\ decomposition}$	0.24	0.45	0.61	1.09	1.70	3.25
Total relative time	54.56	34.80	33.81	41.80	54.00	93.50

Figure 11. *Plastic buckling of cylindrical shell with two holes. Computing time in ANM : regularized Ramberg-Osgood model (Computer used: HP 9000 K 200)*

Truncature order	5	8	10	15	20	30
Step number	56	32	27	23	22	21
$\frac{Fnl\ evaluation}{Kt\ decomposition}$	0.24	0.45	0.61	1.09	1.71	3.26
Total relative time	69.44	46.40	43.47	48.07	59.62	89.46

Figure 12. *Plastic buckling of cylindrical shell with two holes. Computing time in ANM : regularized elastic-perfectly plastic law (Computer used: HP 9000 K 200)*

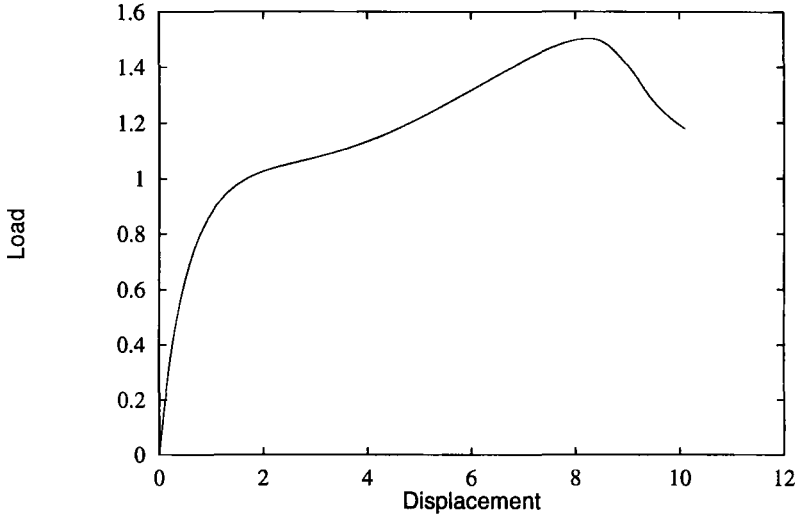

Figure 13. *Regularized Ramberg-Osgood model: load-displacement curve for cylindrical shell; deflexion of the point M is limited at 10*

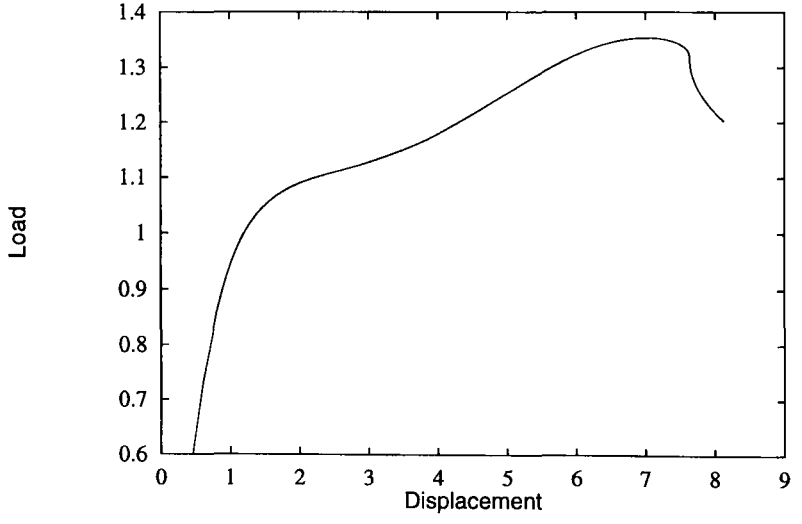

Figure 14. *Regularized elastic-perfectly plastic law: load-displacement curve for cylindrical shell; deflexion of the point M is limited at 8*

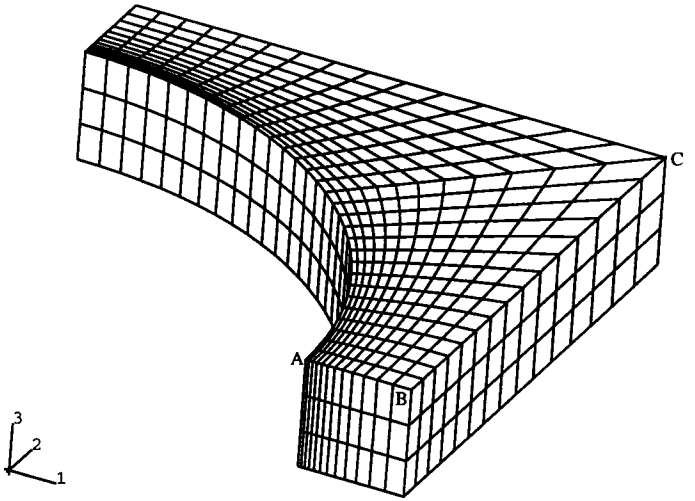

Figure 15. *Plate with a circular cut-out : geometric description*

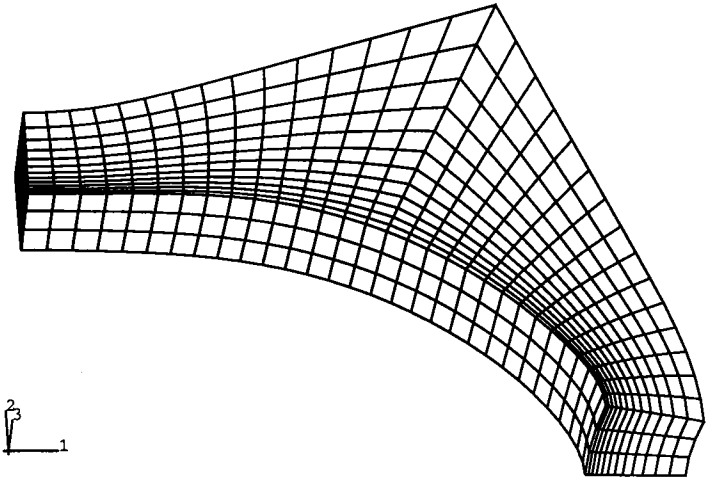

Figure 16. *Plate with a circular cut-out: deformed configuration*

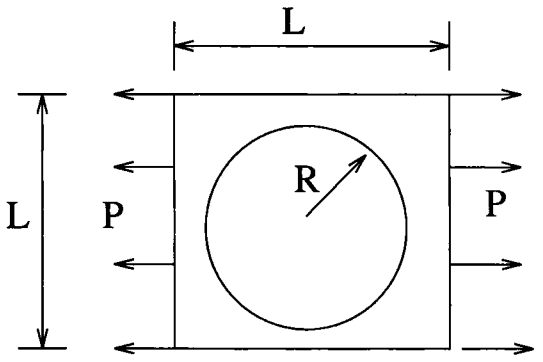

Figure 17. *Plate with a circular cut-out: geometric description*

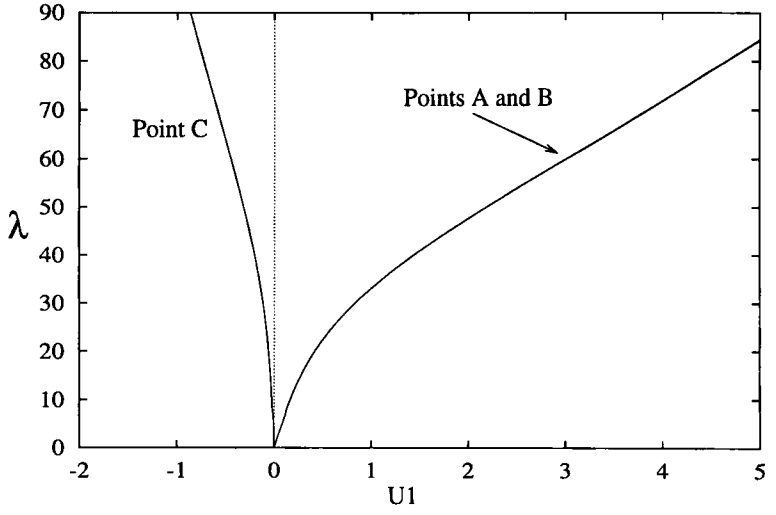

Figure 18. *Load displacement curve at points A, B and C. The current load is* $F = \lambda P$, *with* $P = 0.18$